*Int. J. Electrochem. Sci.*, 10 **(2015)** 9513 - 9527

International Journal of
ELECTROCHEMICAL
SCIENCE
www.electrochemsci.org

# Synthesis of Polyaspartic Acid/Chitosan Graft Copolymer and Evaluation of Its Scale Inhibition and Corrosion Inhibition Performance

*Defang Zeng*[*], *Tengshu Chen, Saijun Zhou*

School of Resource and Environmental Engineering, Wuhan University of Technology, Wuhan 430070, China.
[*]E-mail: 316564419@qq.com

*Received:* 30 June 2015 / *Accepted:* 20 August 2015 / *Published:* 30 September 2015

Polyaspartic acid/Chitosan grafted copolymer (denoted as PASP/CS) was synthesized by using polysuccinimide and Chitosan as the starting materials. Structural characterization was conducted on the reaction product by infrared spectroscopy and $^{1}$HNMR. Static scale inhibition method and dynamic corrosion testing were used to explore the scale and corrosion inhibition performance of PASP and PASP/CS. The experimental results showed that The inhibition efficiency of graft copolymer is 89% for $Ca_3(PO_4)_2$ scale, PASP is only 46% when inhibitor concentration is 8 mg/L. Moreover, the inhibition corrosion efficiency can reach up to 82%, with PASP is 47% when inhibitor concentration is 25 mg/L. When PASP/CS was added to the solution, PASP/CS can change the structure of $CaCO_3$ and $Ca_3(PO_4)_2$ crystal, where the lattice distortion occurs and produced crystal grain size becomes smaller, presenting a dispersed state.

**Keywords:** Chitosan, Corrosion inhibition, Graft copolymer, Scale inhibition

## 1. INTRODUCTION

Circulating cooling water system is widely used in industrial processes [1, 2]. In order to save water resources, it is imperative to apply water treatment agents to process industrial water for slowing down large area corrosion and saving water [3–5]. However, currently used water-treatment agents usually possess unsatisfactory overall performance and cause secondary pollution, which seriously limits their application in industry [6]. In the form of global resources and environmental degradation, green chemistry and green scale inhibitors have become the focus of the research of water treatment chemicals [7–8]. PASP due to the molecule does not contain phosphorus, both scale and corrosion

inhibition performance and good water solubility and can be biodegradable, small environment pollution is a kind of environmental friendly green polymer [9]. Nevertheless, PASP is very poor in scale inhibition of calcium phosphate and poor dispersion capacity for ferric oxide, which seriously restricts it use [10]. To overcome those shortcomings and improve its performance of polyaspartic acid [11], developing green chemistry water pharmacy actively has become imperative.

Chitosan is a partially N-deacetylated derivative of chitin, and is known as the second most abundant biopolymer in nature after cellulose [12]. Recent years, The copolymer scale inhibitor modification with chitosan is a novel scale inhibitor. and research on the graft polymerization of vinyl monomers such as acrylic acid, methyl methacrylate, acrylonitrile, vinylacetate onto chitosan using free radical initiation has been reported [13]. However, the single monomer of the reaction of the formation of the copolymer with the PASP and chitosan has little research on the scale inhibition performance of the circulating cooling water system. Therefore, the major objectives of this work are: Through thermal condensation method, the author has synthesized PSI, and further synthesized graft poly-aspartic acid copolymers with PSI and Chitosan. The impact of graft copolymer on the Scale and Corrosion Inhibition Performance in circulating cooling water was studied, so as to provide theoretical support for the development of the circulating cooling water corrosion and scale inhibition.

## 2. EXPERIMENT

### *2.1 Materials*

Maleic anhydride, polyethylene glycol 6000, urea, sodium bisulfate, Ascorbic acid, anhydrous calcium chloride, ammonium molybdate, were supplied by Sinopharm Chemical Reagent Co.,Ltd, (Shanghai, China). potassium dihydrogen phosphate, calconcarboxylic acid indicator, sodium borate, sodium hydroxide, Urotropine, were supplied by Wuhan Huawei Instrument Co., Ltd, (Wuhan, China). shrimp, Qingdao Fu Yuan Import & Export Co., Ltd, (Qingdao, China).

Bruker DRX-400 Nuclear Magnetic Resonance, 602 Constant temperature oil bath pot, RCC-Ⅲ rotary coupon corrosion tester, JSM-5610LV scanning electron microscope (SEM), 722 grating spectrophotometer were used in the present research. A3 carbon steel of the following chemical composition(%):C(0.140), Mn(0.350), Si(0.300), S(0.045), P(0.040) and balance Fe.

### *2.2 Synthesis of polyaspartic acid–chitosan grafted copolymer*

29.4g Maleic anhydride and 70ml deionized water were added into the beaker and dissolved in 45℃ water bath pot [14].18g urea and 30ml deionized water were added and slowly dissolved at room temperature. a dropper was used to slowly add to the three-necked flask with Maleic anhydride, which was placed in the 100℃ oil bath pot and heated for 1h. And then, 5.88g sodium bisulfate and certain amount of polyethylene glycol 6000 were added and the oil bath temperature was raised to 180℃. followed 3h of reaction, it was taken out and cooled to room temperature. Absolute ethanol was added and stirred to get the red-brown sticky solid. The supematant was removed and placed in the drying

cabinet, where the obtained red-brown solid was polysuccinimide. Relevant synthetic reaction is expressed in Fig. 1.

Certain amounts of PSI and water were mixed at room temperature. Next, A proper amount of as dried chitosan and acetic acid were mixed was slowly added to the mixture under stirring. until the reaction completely became claybank solution. Absolute ethanol was added and stirred to get the claybank sticky solid. The supematant was removed and placed in the drying cabinet, where the obtained claybank solid was polyaspartic acid-chitosan (PASP/CS). Relevant synthetic reaction is expressed in Fig. 2.

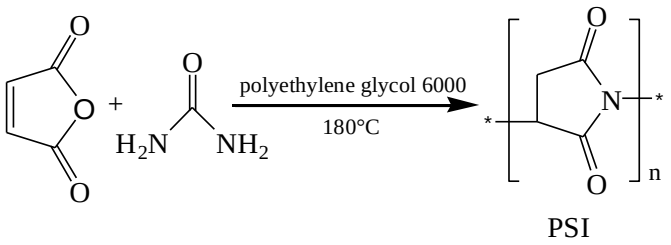


**Figure 1.** Synthesis route of PSI.

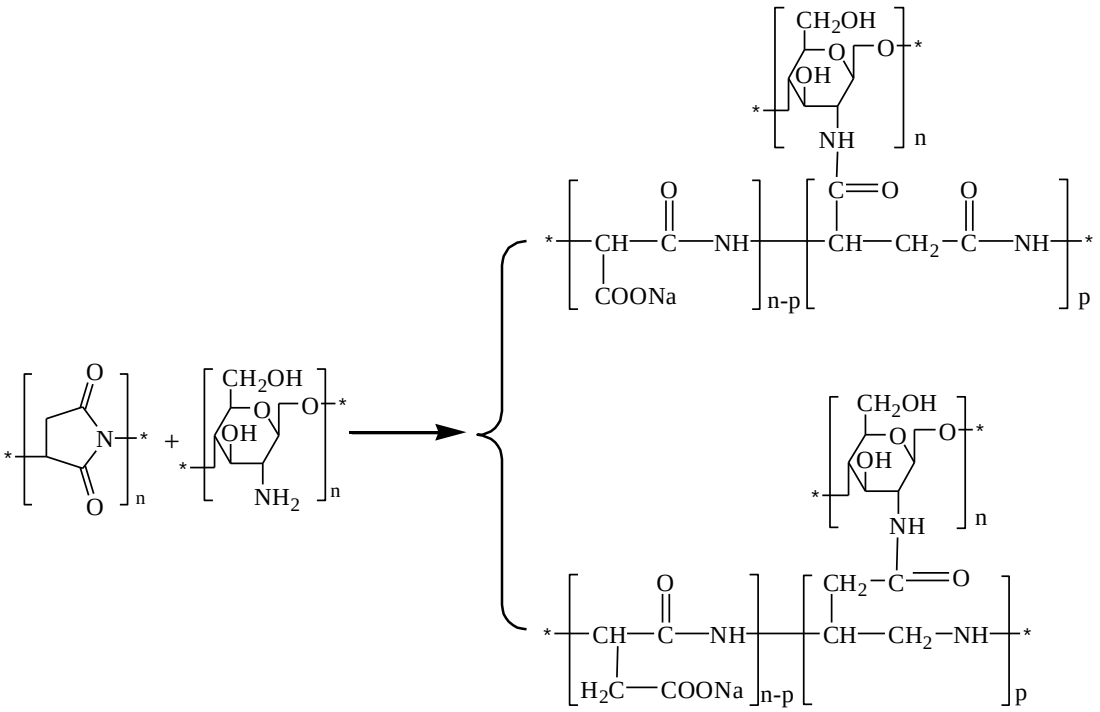

**Figure 2.** Synthesis route of PASP/CS graft copolymer.

*2.3 Inhibition performance of PASP/CS copolymer against $CaCO_3$ scale*

Static scale inhibition tests were conducted according to China National Standard method (GB/T16632-2008) to evaluate the scale inhibition efficiency of PASP/CS against $CaCO_3$ scale [15]. taking $CaCl_2$ and $NaHCO_3$ solid to prepare experiment water of $\rho(Ca^{2+})$=240 mg/L, $\rho(HCO^{3-})$=366

mg/L, The time for water bath is 10 hours. The inhibition efficiency of the scale inhibitor against $CaCO_3$ scale was calculated as according to Eq. (1)

$$\eta_{CaCO_3} = \frac{\rho_1 - \rho_0}{\rho_2 - \rho_0} \times 100 \quad (1)$$

Where $\rho_0$、$\rho_1$ is the volume of EDTA in the absence and presence of scale inhibitor in to-be-tested solution. $\rho_2$ is the mass volume of EDTA all in to-be-tested solution.

### *2.4 Inhibition performance of PASP/CS copolymer against $Ca_3(PO_4)_2$ scale*

$Ca_3(PO_4)_2$ inhibition tests were carried out in artificial cooling water. The test solution containing 240 mg/L $CaCl_2$ (as $CaCO_3$), 5 mg/L $KH_2PO_4$ and a certain amount of inhibitor was pH adjusted to 9.0 with borax and was incubated at 80 °C for 10 h. The solution was filtered and the $PO_4^{3-}$ concentration in the filtrate was detected by ammonium molybdate spectrophotometric method. The inhibition efficiency of $Ca_3(PO_4)_2$ was calculated according to Eq. (2).

$$\eta_{Ca(Po_4)_2} = \frac{\beta_1 - \beta_0}{\beta_2 - \beta_0} \times 100 \quad (2)$$

Where： $\beta_0$, $\beta_1$is the absorbance of $PO_4^{3-}$ in the absence and presence of scale inhibitor in to-be-tested solution. $\beta_2$ is the mass absorbance of all in to-be-tested solution.

### *2.5 Weight loss studies for corrosion inhibition efficiency*

The corrosion inhibition efficiency of graft copolymer was measured by weight loss of rotating hung steel slices [16]. A3 carbon steel coupon (50×25×2 $mm^3$) was used as the corrosion object. The inhibitors were added into laboratory circulating cooling water. The coupon was placed in the (45±1) ℃ inhibitor test the water and rotated in 75 r/min, which was then removed after 72 h. The blank test without inhibitors was also operated. The corrosion rate ν and the corrosion inhibition efficiency λ were calculated by using the following equations:

$$\nu = \frac{8760 \times \left[(m_0 - m_1) - \Delta m\right]}{S \times T \times D} \quad (3)$$

$$\lambda = \frac{\nu_0 - \nu}{\nu_0} \times 100 \quad (4)$$

In Eqs. where $m_0$ and $m_1$ is the mass of carbon steel hung slices before and after test; Δm is the mass loss of carbon steel hung slices caused by washing in acid. S is the surface area of carbon steel hung slice. T is testing time. D is density of carbon steel hung slices. $\nu_0$ and ν is annual corrosion rate in the absence and presence of scale inhibitor. λ is corrosion inhibition efficiency .

### *2.6 Electrochemical test*

The instrument used in the electrochemical test is CHI660D electrochemical workstation (Shanghai Chenhua Instrument Co. Ltd, China). The potential range of impedance test was 10 mV, and frequency range 10 kHz to 10 MHz, The scan rate of Tafel potential test was 0.5 mV/s, and the

scanning range was form +250 to -250 mV. The test temperature was 25, and test water was 3.5% NaCl solution. Three electrode polarization method was used in the experiment. A3 carbon steel sheet as the working electrode, saturated calomel electrode (SCE) as a reference electrode, platinum sheet as a counter electrode. A3 carbon steel for the experimental materials [17]. The polarization curves of A3 carbon steel were obtained by using Tafel technology in the 3.5% NaCl solution of the blank and the different concentrations of corrosion and scale inhibitor, The percentage inhibition efficiency (η) was computed from corrosion current density (Icorr ) values using the relationship as the following Equation (5):

$$\eta = \frac{I_{corr} - I'_{corr}}{I_{corr}} \times 100\% \qquad (5)$$

Where in Icorr and I′corr are the corrosion current density without and with inhibitor, respectively, mA/cm$^2$.

## 3. EXPERIMENTAL RESULTS AND CONCLUSIONS

### *3.1 IR spectroscopy characterization of PASP and PASP/CS*

FT-IR spectra of chitosan, Polyaspartic acid and Polyaspartic acid/chitosan are shown in Fig. 3. Characteristic peaks assignment of chitosan (Fig. 3a) are the broad band around 3428 cm$^{-1}$ attributed to -OH and -NH stretching vibration. The weak band at 2920 and 2867 cm$^{-1}$ was the characteristic absorbance peak of -CH. The peak at 1634 cm$^{-1}$ was ascribed to amide II band, C-O stretch of acetyl group, the absorption peak at 1589 cm$^{-1}$ assigned to -$NH_2$ bending vibration. Additionally, the absorption peaks of symmetric stretching of the C-O-C appeared at 1157 cm$^{-1}$, 1079 cm$^{-1}$ and 1026 cm$^{-1}$ [18]. The IR spectral band of Polyaspartic acid (Fig. 3b): The characteristic peaks at 3420 and 1601 cm$^{-1}$ can be attributed to the stretching and bending vibration of N-H in amide, respectively. The peak at 1610 cm$^{-1}$ was ascribed to C=O, whereas the peak at 1398 cm $^{-1}$ corresponds to the strong signal of C-N [19].

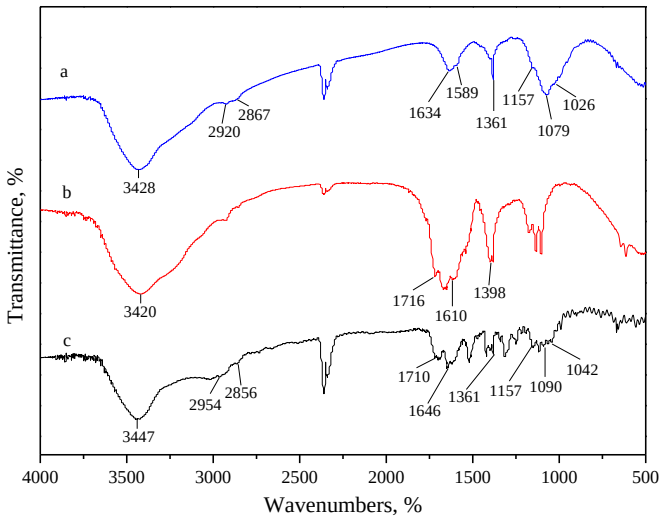


**Figure 3.** FT-IR spectra of CS (a), PASP (b), and PASP/CS (c).

As shown in Fig. 3c, Compared with chitosan and Polyaspartic acid, new bands at 1646 $cm^{-1}$ was ascribed to amide II for PASP/CS were also observed, In addition, the peak at 1589 $cm^{-1}$ of the primary amine became weak which meant amino has been partly substituted. The above FTIR analysis clearly indicates that the COOH group of Polyaspartic acid has been successfully reacted with $NH_2$ group of chitosan main chain to form amide linkage. Hence, the structure of PASP/CS was confirmed [20].

### *3.2 $^1$H NMR spectrum of Polyaspartic acid–chitosan grafted copolymer*

The $^1$ H NMR spectra of chitosan, Polyaspartic acid and Polyaspartic acid/chitosan conjugate were given in Fig. 4. Proton assignment of chitosan in Fig. 4a，δ= 4.75 ppm is chemical shift of the acetal proton (C-H) of glucosamine ring, δ= 3.27 ppm for –CH-$NH_2$ protons ($H^2$), δ= 3.92–3.72 ppm for ($H^3$, $H^4$, $H^5$ and $H^6$) protons of glucosamine ring, δ= 3.27 ppm appear for chemical shifts of ($H^2$) proton and up field，δ = 2.04 ppm for (NHCO-$CH_3$) acetamido protons [21]. δ= 2.5 ppm appears for chemical shift of the internal standard. Proton assignment of Polyaspartic acid shown in Fig. 4b, It can be seen that δ = 2.76 ppm is attributed to the characteristic peak of methylene, and the δ = 4.45 ppm is ascribed to the peak of amide [22]. Compared with chitosan and Polyaspartic acid, the characteristic proton signals of PASP/CS (Fig. 4c), appeared at δ= 5.55 ppm (s) is due to N-H proton of amide linkage which is formed between $NH_2$ group of chitosan and COOH group of Polyaspartic acid, The $^1$ H NMR spectra confirm the formation of new amide linkage between COOH group of Polyaspartic acid and $NH_2$ group of chitosan. Respectively, This result was also consistent with the FT-IR results we discussed. Hence, the structure of PASP/CS was further confirmed.

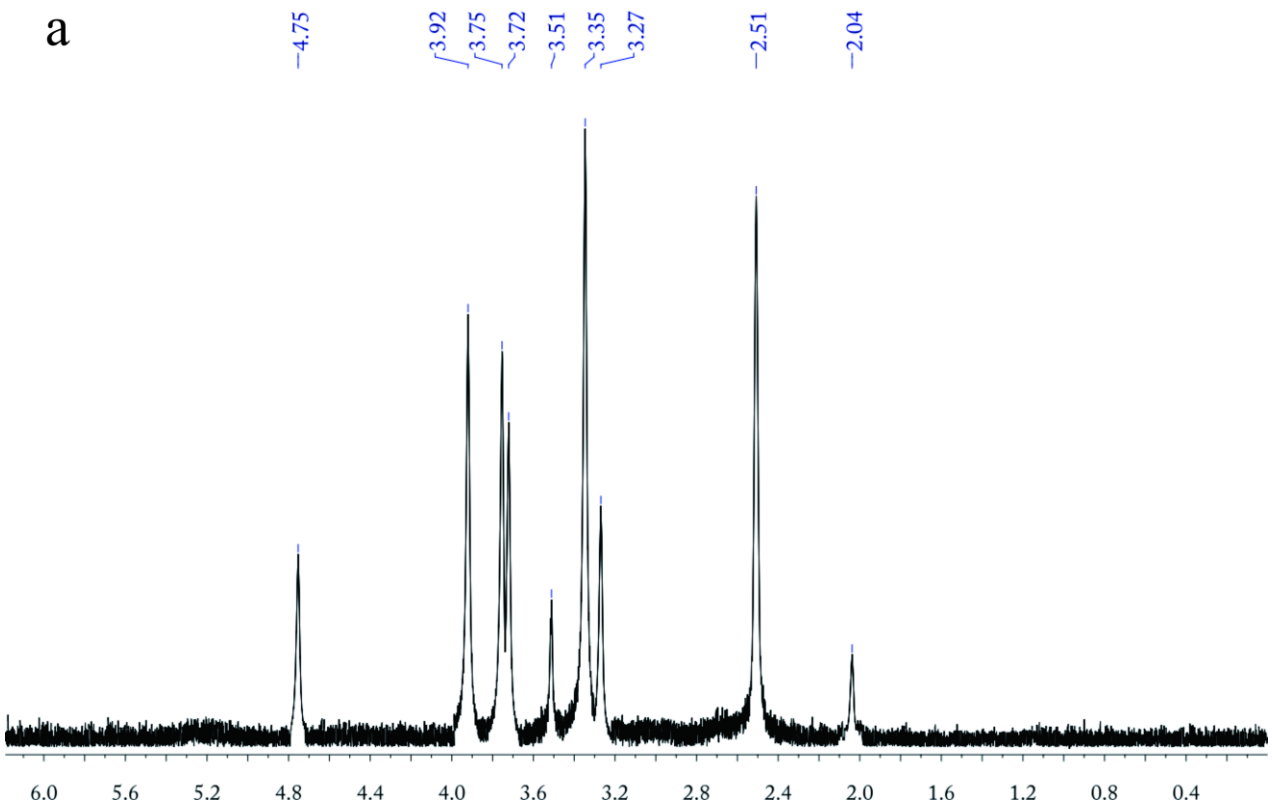

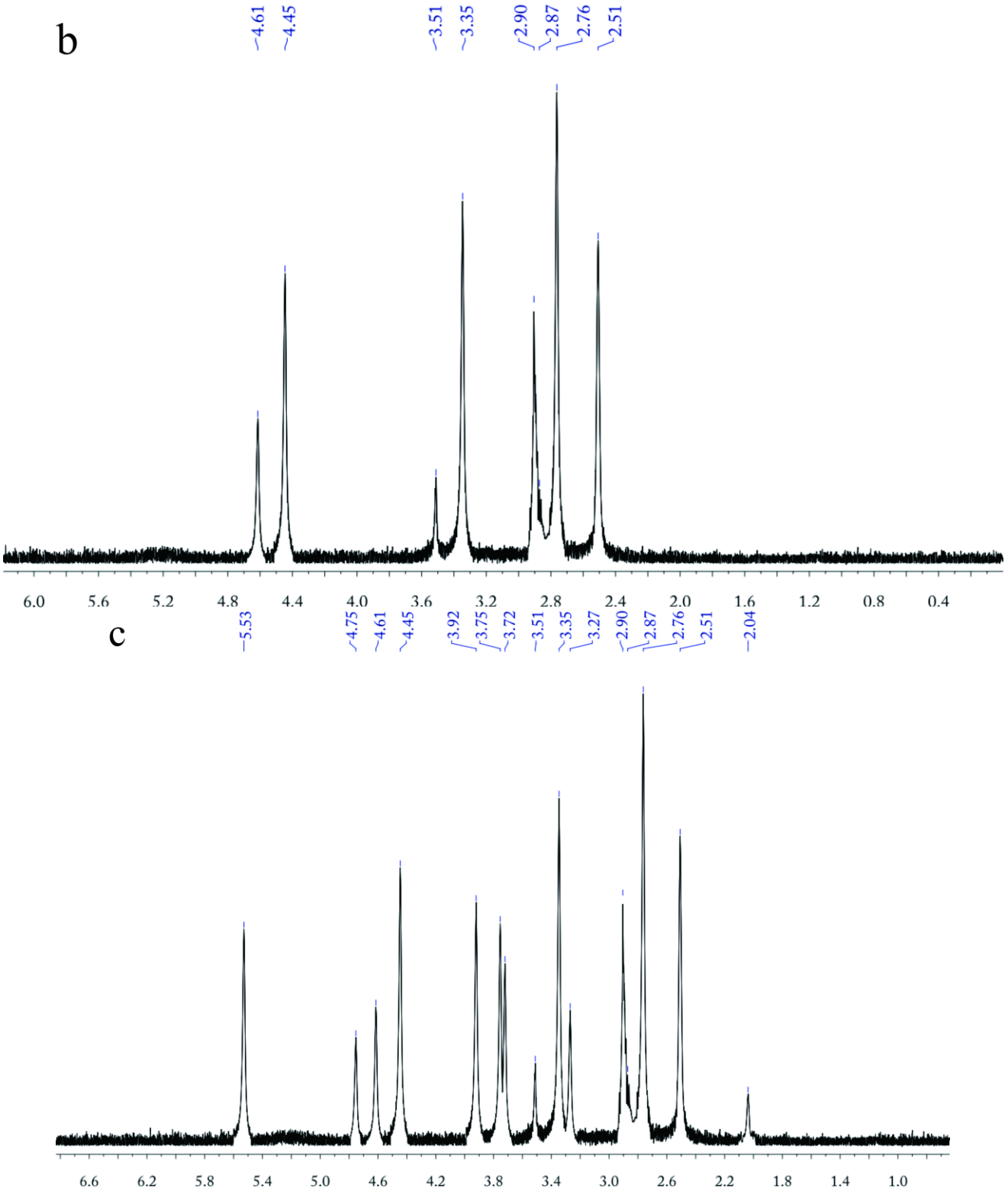


**Figure 4.**[1] HNMR spectra of CS (a), PASP (b), and PASP/CS (c).

*3.3 The inhibition efficiency of PASP/CS grafted copolymer against $CaCO_3$ scale*

Fig.5 shows the variation of their inhibition efficiency against $CaCO_3$ scale with a different concentration of the scale inhibitor. The concentration of $Ca^{2+}$ is 240 mg/L, the heating time is10 h.

The scale inhibition efficiency increased with the increase of PASP/CS and PASP concentration. When PASP concentration was at 8 mg/L, the inhibition efficiency was 68%, the maximum inhibition efficiency was 92% when PASP/CS concentration was 8 mg/L. When the concentration continues to increase, the scale inhibition rate has not changed. It shows that the performance of the grafted copolymer against $CaCO_3$ scale was better than PASP. The excellent inhibition ability of PASP/CS against $CaCO_3$ scale may relate to its simultaneous possession of carboxylic ion, hydroxyl group and Nitrogen, oxygen atoms of amide in lone pair of electrons structure. These structures can effectively adsorb the scale nuclei, reduce its growth rate, and delay the formation of precipitation [23].

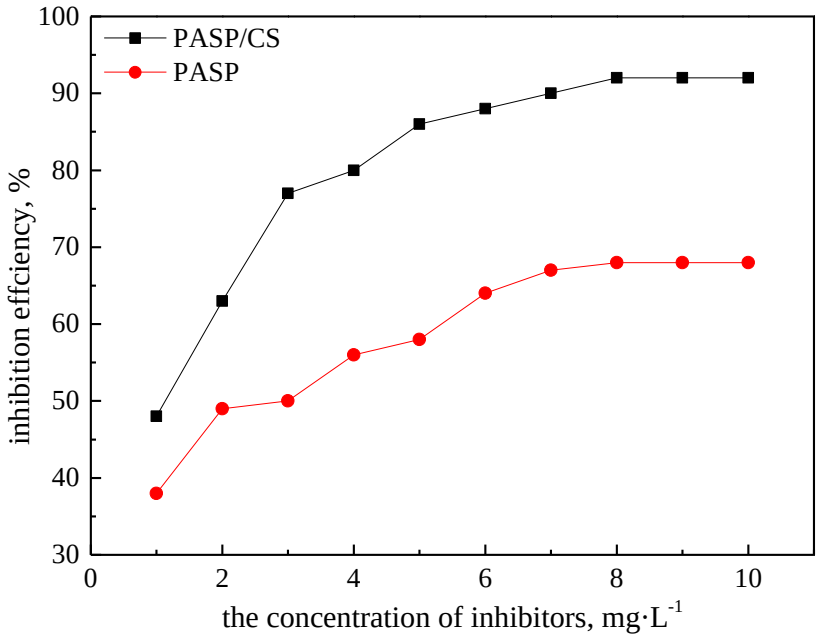


**Figure 5.** The inhibition efficiency of PASP/CS grafted copolymer against $CaCO_3$.

### *3.4 Influence of concentration of $Ca^{2+}$ on inhibition efficiency of PASP/CS grafted copolymer*

$Ca^{2+}$ was often referred to an important factor for iron corrosion [24]. The influence of $Ca^{2+}$ concentration on the inhibition efficiency as shown in Fig.6. As the calcium concentration increased, inhibition efficiency gradually decreased. When the $Ca^{2+}$ was 350 mg/L, inhibition rate of PASP/CS and PASP respectively were 87% and 69%, when the calcium ion concentration was greater than 350 mg/L, the inhibition efficiency drastically reduced. When the calcium ion concentration was 500 mg/L, the inhibition efficiency of PASP/CS and PASP respectively were 58% and 35%, this is because the calcium carbonate scale increases with the increasing concentrations of calcium ions. Nonetheless, the inhibition efficiency of PASP/CS grafted copolymer against $CaCO_3$ scale exceeded PASP. This may be because the introduction of the chitosan and its functional groups on the side chain of the grafted copolymer enhances the complexing abilities for $Ca^{2+}$.

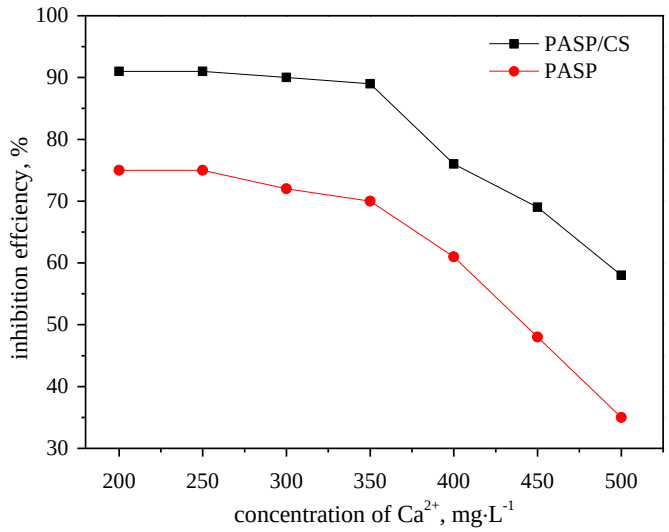


**Figure 6.** Influence of $Ca^{2+}$ concentration on inhibition efficiency of PASP/CS.

*3.5 Influence of the pH on inhibition efficiency of PASP/CS grafted copolymer*

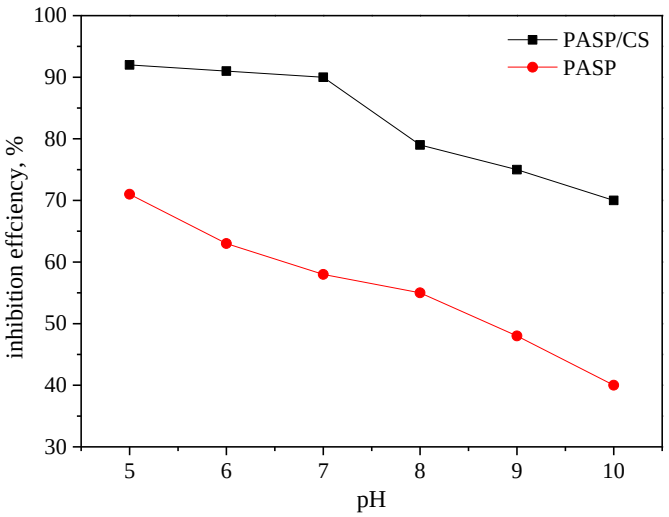


**Figure 7.** Influence of pH on inhibition efficiency of PASP/CS grafted copolymer.

The scale inhibition efficiencies at different pH are shown in Fig.7. The higher the pH was, the lower the scale inhibition efficiency was, the PASP/CS and PASP were all sensitive to high pH value. Comparison of scale inhibition experiments, the scale inhibition rate of PASP/CS was higher than that of PASP. When the solution was acidic, PASP/CS and PASP both reflect the superior scale inhibition performance. the scale inhibition performance of PASP/CS was higher than that of PASP 27%.When the solution was alkaline, the scale inhibition rate of PASP/CS and PASP was decreased. The scale inhibition performance of PASP/CS is still relatively high. Compared with the PASP, the increase of 26%, PASP/CS is suitable for the water treatment system in the range of pH 5~8, and its scale inhibition rate is above 80%.

When the solution is acidic, the ion in the system is $HCO^{3-}$, the reaction of $CO_3^{2-}$ with $Ca^{2+}$ is little. So as to reduce the speed of $CaCO_3$ precipitation, and the higher PASP/CS scale inhibition rate [25]. With the increase of pH value of solution, The $HCO^{3-}$ in the system is constantly changing to $CO_3^{2-}$, thus speeding up the speed of $CaCO_3$ precipitation. PASP/CS scale inhibition rate began to decline.

### *3.6 Influence of concentration of PASP/CS grafted copolymer on inhibition efficiency against $Ca_3(PO_4)_2$ scale*

Fig. 8. shows the inhibition efficiency of PASP/CS grafted copolymer against $Ca_2(PO_4)_3$ scale. $Ca^{2+}$ was maintained at 240 mg/L, $PO_4^{3-}$ 5 mg/L, of which the pH value is 9. Place in constant temperature 80 ℃ for 10 h to study the impact of PASP and PASP/CS of different concentrations on the scale inhibition efficiency calcium phosphate. The scale inhibition efficiency of both PASP and PASP/CS increased as the concentration of scale inhibitor increased. PASP reached to the maximum 46% when the concentration was 8 mg/L, while the scale inhibition efficiency reached to 89% when its concentration was 8 mg/L. After that, there was no significant increase in scale inhibition efficiency as the concentration continued to grow. Meanwhile, it could be found that the anti-scaling performance of PASP/CS was well above the PASP for $Ca_2(PO_4)_3$ scale. The results indicates that PASP/CS can effectively improve the inhibition efficiency of calcium phosphate scale, This improvement is due to the incorporation of chitosan. Compared with PASP, after the hydrophilic carboxyl groups are substituted by the hydrophobic hydroxyl groups in PASP/CS, the adsorption of PASP/CS on $Ca_3(PO_4)_2$ is enhanced, and therefore the inhibition efficiency is improved [26].

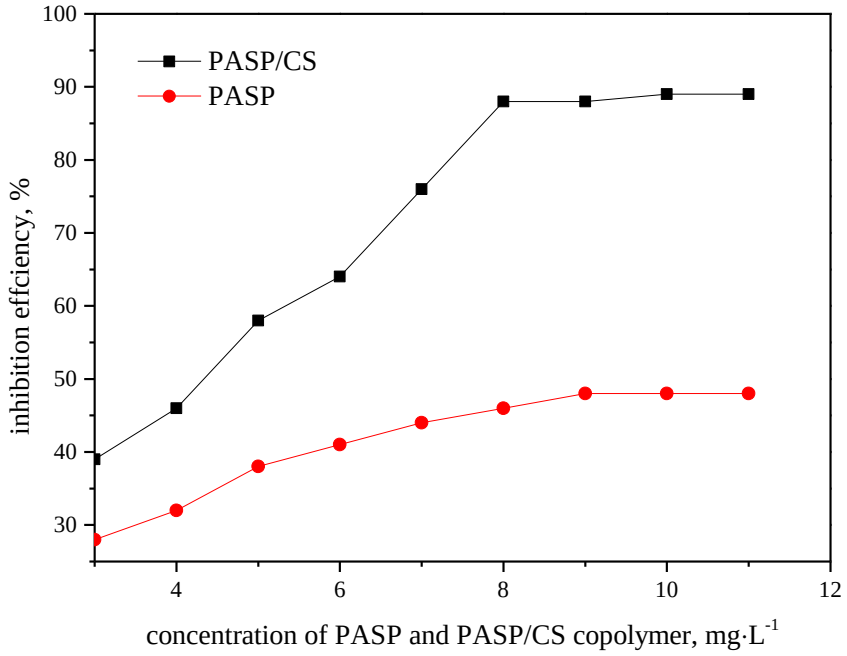


**Figure 8.** The inhibition efficiency of PASP/CS against $Ca_2(PO_4)_3$

*3.7 Studies on Corrosion Inhibition Performance of PASP/CS and PASP*

A3 steel was placed in the (45±1) ℃ test water of scale inhibitor and rotated in 75 r/min. Coupon after 72 h was removed, and corrosion rate was measured by weight loss method so as to study the impact on inhibition performance of PASP and PASP/CS. As shown in Fig.9, the Corrosion inhibition performance of both PASP/CS and PASP were improved as the concentration increased. When the PASP/CS concentration is at 25 mg/L, the corrosion inhibition efficiency reached to the maximum 82%, and the inhibition efficiency of PASP was 47%, which may be due to the introduced polar groups enhance the adsorption of metal, making these molecules more densely adsorbed on the metal surface, while the hydrophobic groups on the other side act together with the hydrophilic groups and form a dense protective film on metal surface. It can hinder water and oxygen from dispersing to the metal, so as to play a role in corrosion inhibition [27, 28].

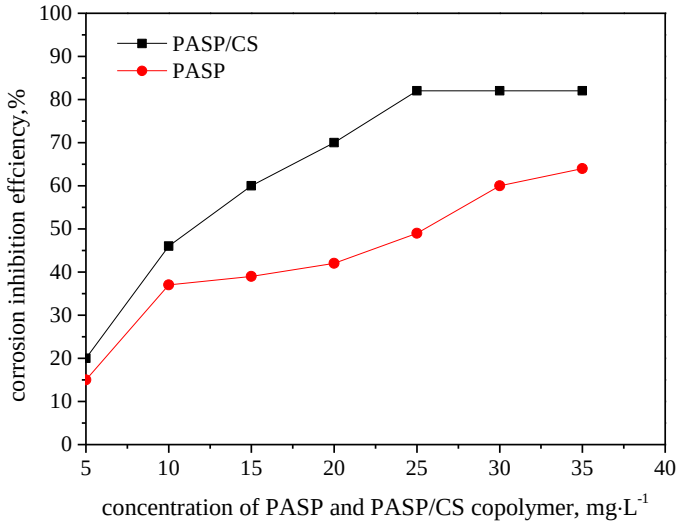


**Figure 9.** Influence of PASP and PASP/CS concentration on corrosion inhibition efficiency

*3.8 Polarization curve*

Using 3.5% NaCl solution and adding different concentrations of PASP/CS as the system, the polarization curve test was carried out. Room temperature is 25. Polarization curve test results are shown in figure 10. The corrosion potential of the electrode in the polarization curve of the PASP/CS and without PASP/CS is compared. After the addition of PASP/CS, the cathode and anodic polarization currents were inhibited by different degrees. The slope of anodic polarization curve is obviously increased, and the anode current decreases obviously. The change of the slope of the cathode polarization curve is small, and the cathode current is not obvious. That shows that PASP/CS is a kind of corrosion inhibitor which is based on the inhibition of anodic polarization. With the increase of the concentration of PASP/CS, the corrosion potential of the electrode is gradually shifted to the positive direction, and the corrosion current density decreases gradually. This shows that PASP/CS has a certain inhibition effect on the cathode of electrochemical corrosion process [29], the corrosion process of the anodic inhibition gradually increased.

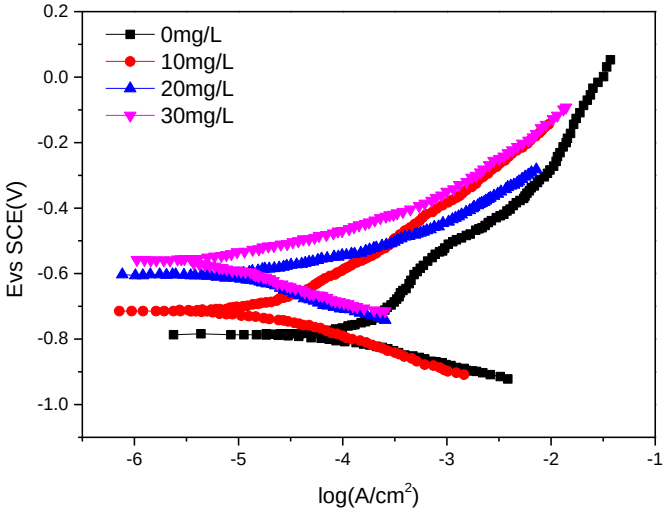


**Figure 10.** Polarization curves of carbon steel in different concentrations of PASP/CS

Tafel extrapolation using by the measured polarization curve cathode and anodic polarization curves in Tafel region in the straight part of the extension, the corrosion current density of the carbon steel electrode can be obtained without adding PASP/CS and adding different concentration of PASP/CS. By the polarization curve of Figure 10, the electrochemical parameters of PASP/CS at different concentrations can be obtained by using the strong polarization region, The corrosion kinetic parameters such as cathodic Tafel slopes ($b_c$), anodic Tafel slopes ($b_a$), corrosion current density (Icorr) were generated from the electrochemical workstation. The results are shown in table 1.

**Table 1.** Polarization curves electrochemical parameter and inhibition efficiency under PASP/CS

| PASP/CS(mg/L) | $E_{corr}$(V) | $b_c$(V/decade) | $b_a$(V/decade) | $i_{corr}$(mA/m$^2$) | η（%） |
|---|---|---|---|---|---|
| 0 | -0.887 | 9.514 | 3.080 | 0.1463 | — |
| 10 | -0.792 | 9.653 | 6.470 | 0.07827 | 46.50 |
| 20 | -0.681 | 9.762 | 10.191 | 0.04263 | 70.86 |
| 30 | -0.635 | 10.480 | 12.189 | 0.0255 | 82.57 |

From table 1, With the increase of PASP/CS concentration, the corrosion potential increases, the $b_c$ and $b_a$ of the cathode and anodic polarization curves increases gradually, the corrosion current density decreases, and the corrosion inhibition efficiency of PASP/CS is gradually increased [30]. The results of polarization curve test and rotating hanging plate method are consistent with the experimental results.

*3.9 Electrochemical impedance spectroscopy*

Using 3.5% NaCl solution and adding different concentrations of PASP/CS as the system, Electrochemical impedance test results are shown in figure 11. Under different concentrations of PASP/CS, the impedance spectra obtained have similar characteristics. With the increase of PASP/CS concentration, the semicircle radius increases, Charge transfer resistance (Rct) on the surface of the steel sheet is increasing. For corrosion inhibition system, Rct is a reflection of the resistance of the corrosion inhibitor to the metal surface of the metal surface. Rct is a reflection of the resistance of the metal surface coating to metal ionization process, or the corrosion reaction rate. The greater the value of Rct, the greater the resistance of the metal ions, the smaller the corrosion rate of metals [31], It is indicated that the PASP/CS molecules formed a good protective film on the surface of carbon steel, which replaced the water molecules that cover the surface of carbon steel.

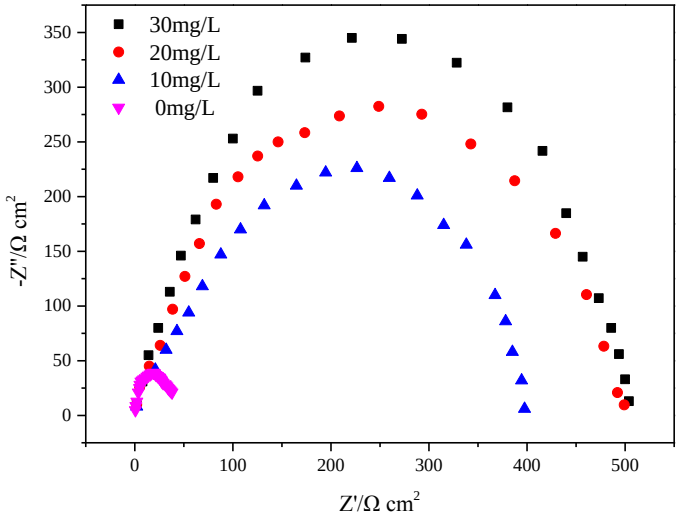


**Figure 11.**Impedance spectra of carbon steel in different concentrations of PASP/CS

*3.10 SEM pictures of $CaCO_3$ and $Ca_3(PO_4)_2$ crystals in the absence and presence of PASP/CS grafted copolymer*

In order to observe changes in $CaCO_3$ and $Ca_3(PO_4)_2$ crystals after adding PASP/CS inhibitor more intuitively, so as to analyze inhibition mechanism, the experimental temperature was set at 80 ℃ with constant temperature concentration for 10 h. Scanning electron microscope was conducted on the concentrated scale after filtered and dried. In the experiment, the scan voltage is set at 25 kv with a magnification of 1000 times. SEM of $CaCO_3$ and $Ca_3(PO_4)_2$ with or without adding PASP/CS inhibitor is shown in Fig.12. Without adding PASP/CS (A), most calcium carbonate scales were regular crystal diamond-shapes with compact crystal structure and larger volume. After adding PASP/CS (B), the formed $CaCO_3$ scale crystals were no longer diamond-shaped with lattice distortion, in which shapes became irregular, and the edges were relatively smooth with loose crystals. $Ca_3(PO_4)_2$ crystal particles without adding PASP/CS (C) are flocculent micelles in macroscopic, microscopic mixture of amorphous, polycrystalline. After adding PASP/CS (D), the surface of colloidal particles and

microcrystalline particles can obviously change the loose divergence of calcium phosphate particles and make calcium phosphate more difficult to precipitate [32].This is because the carbonate ions and phosphate ions and calcium ions combined by collision and grow into regular diamond-shaped crystals. After adding PASP/CS inhibitor, since structures were damaged which could not grow in original direction, and shapes became irregular and dispersed, formed crystals become smaller with loose structure, so that the formed scales will easily be washed away [33].

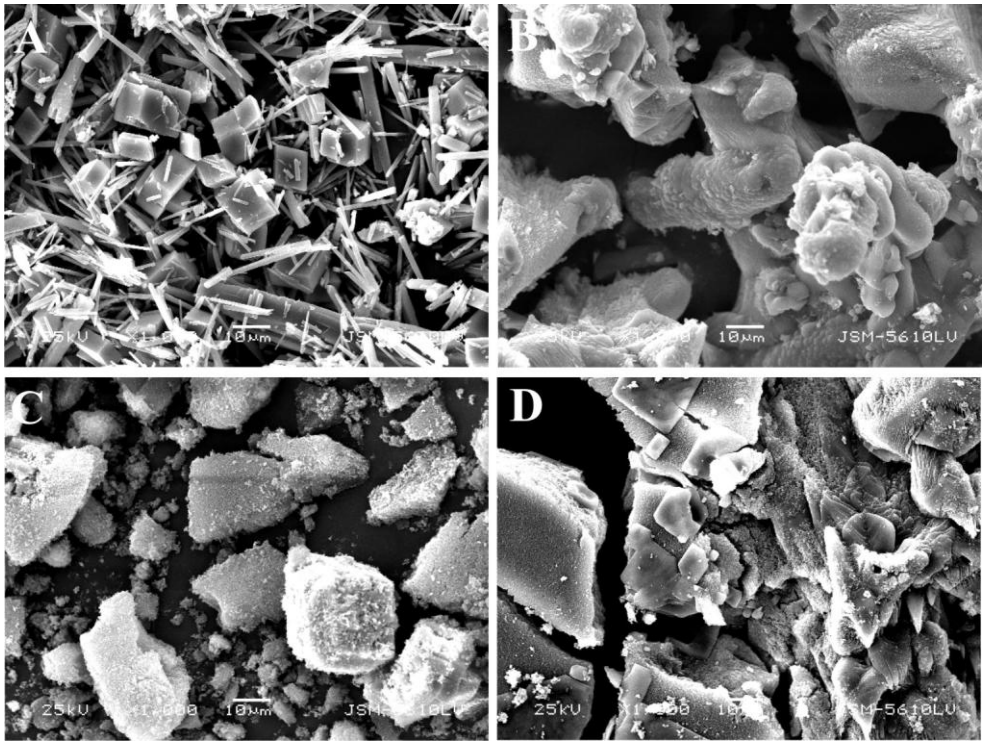


**Figure 12.** SEM pictures of $CaCO_3$ (A) and $Ca_3(PO_4)_2$ (C) without grafted copolymer, $CaCO_3$ (B) and $Ca_3(PO_4)_2$(D) with grafted copolymer.

## 4. CONCLUSION

A novel scale inhibitor Polyaspartic acid/Chitosan graft copolymer was prepared. It could be found that the graft copolymer possesses very good scale inhibition performance for $CaCO_3$ and $Ca_3(PO_4)_2$ scales by static scale inhibition method. Its corrosion inhibition and scale inhibition performance for $Ca_3(PO_4)_2$ scale have improved significantly compared with PASP through testing. PASP/CS has a certain inhibition effect on the cathode of electrochemical corrosion process, The corrosion process of the anodic inhibition gradually increased. In addition, the graft copolymer could destroy the growth habit of the crystal and lead to crystal aberration.

ACKNOWLEDGEMENTS
This work was financially supported by the Chinese Technology Innovation Foundation for Technology Based Small and Medium Sized Enterprises (10C26214202268).Thank you for helping us with the project.

**References**


1. Saad Ghareba, Sasha Omanovic, *Corros.Sci*. 52 (2010) 2104.
2. R. Touir, N. Dkhireche, M. Ebn Touhami, *Desalination*. 249 (2009) 922.
3. I. Andijani, S. Turgoose, *Desalination*. 123 (1999) 223.
4. M.H. Al-Malack, S.Y. Sheikheldin, *Water Res*. 35 (2001) 3283.
5. N. Abdel-Aal, K. Sawada, *J. Cryst. Growth*. 256 (2003) 188.
6. W.Chen,P.L.Shu,D.L.Tian, *Desalination*. 249 (2009) 1.
7. J.C. Dong, J.Y. Seung, G.K. Jung, *Mater.Sci. Eng*. 335 (2002) 228.
8. F.S. De Souza, A. Spinelli, *Corros. Sci*. 51 (2009) 642.
9. J.H. Guo, S.J. Severtson, *Ind. Eng. Chem. Res*. 42 (2003) 3480.
10. M.M. Kunjapur, W.H. Hartt, S.W. Smith, *Corros. Sci*. 43 (1987) 674.
11. Y.X. Zhang, J.H. Wu, S.C. Hao, M.H. Liu, *Chin. J. Chem. Eng*. 15 (2007) 600.
12. N. Nakada, T. Tanishima, H. Shinohara, K. Kiri, H. Takada, *Water Res*. 40 (2006) 3297.
13. Xiaorui Guo, Fengxian Qiu, Ke Dong, Xin Zhou, Jing Qi, Yang Zhou, Dongya Yang. *Journal of Industrial and Engineering Chemistry*. 18 (2012) 2177.
14. H.J. He, C.X. Xu, Y.H. Wang, S.X. Zhan, Y.Y. Ma, Y.P. Yang, *Industrial Water Treatment*. 23 (2003) 33.
15. T. Kumar, S. Vishwanatham, S.S. Kundu, *J. Pet. Sci. Eng*. 71 (2010) 3.
16. R. Touir, M. Cenoui, M. El Bakri, M. Ebn Touhami, *Corros. Sci*. 50 (2008) 1530.
17. De-fang Zheng, Wei Zhang, Dan Hu, Shui-sheng Zhang, Fu-jun Ding, *Contemporary Chemical Industry*. 40 (2011)10.
18. Kubota, N., & Eguchi, Y. Facile, *Polymer Journal*. 29 (1997) 123.
19. Jinyong Li, Yongbo Ao, Defang Zeng, *Appl Chem. Ind*. 37 (2008) 770.
20. Santosh Kumar, Joonseok Koh , Hyerim Kim , M.K. Gupta, P.K. Dutta, *International Journal of Biological Macromolecules*. 50 (2012) 493.
21. Chen, X. G., & Park, H. J. *Carbohydrate Polymers*. 53 (2003) 355.
22. Ben Zhang, Dapeng Zhou, Xiaogai Lv, Ying Xu , Yuanchen Cui, *Desalination*. 327 (2013) 32.
23. Jiuying Feng, Lijun Gao, Rizhen Wen, Yiyi Deng, Xiaojun Wu, Shulin Deng. *Desalination*.345 (2014) 72.
24. A. Sander, B. Berghult, A. Elfstrom Broo, E. Lind Johansson, T. Hedberg, *Corros. Sci*. 38 (1996) 443.
25. Jiang Yuan, Study on Synthesis and scale inhibition of hydroxy - containing poly - aspartate derivatives, *Heilongjiang University*. (2013).
26. Andrea Niedermayr, Stephan J. Köhler, Martin Dietzel, *Chemical Geology*. 340 (2013) 105.
27. A.M.Abdel-Gaber, B.A.Abd-El-Nabey, E.Khamis, D.E.Abd-EI-Khalek. *Desalination*.278 (2011) 337.
28. P.K.Gogoi, B.Barhai. *International Journal of Electrochem Science*. 6 (2011) 136.
29. Ramazan Solmaz, *Corros. Sci*. 81 (2014) 75.
30. J.R. Xavier, R. Nallaiyan, *J. Solid State Electrochem*. 16 (2012) 391.
31. Lu Xiang-hong, Zhao Guo-xian, Zhang Jian-bing, Xie Kai-yi, *Journal of University of Science and Technology Beijing*,32 (2010) 208.
32. LAI Xiaofang，WANG Jide，XU Xinliang，GUO Jingyu, *FINE CHEMICALS*. 3 (2013) 113.
33. Ying Xu, Ben Zhang, Linlin Zhao, Yuanchen Cui. *Desalination*. 311 (2013) 156.